

INVESTIGATION OF ENVIRONMENTAL EFFECTS ON INTRINSIC AND GALVANIC CORROSION OF MILD STEEL WELDMENT IN CO₂ ENVIRONMENT

Lei Huang*, Bruce Brown, Srdjan Nestic

Institute for Corrosion and Multiphase Technology (ICMT)
Department of Chemical and Biomolecular Engineering
Ohio University, 342 W. State St., Athens, OH 45701

ABSTRACT

Localized corrosion of carbon steel welds has been thought to arise primarily from galvanic effects due to compositional differences between the deposited weld metal, the parent steel, and the heat affected zone induced by the welding process. The location and morphology of the preferential corrosion is influenced by a complex interaction of environmental parameters.

The effects of salt concentration and temperature on intrinsic and galvanic corrosion of the non-alloyed standard carbon steel weldment in CO₂ environments have been investigated using different types of electrochemical techniques. Experimental results show that for the non-alloyed standard weldment, the intrinsic corrosion rates of parent metal, heat affected zone (HAZ) and weld metal are not significantly different, but the corrosion of weld metal becomes worse and the parent metal is protected due to the galvanic effects between the segments. The experimental results also show that an increase of salt concentration (1~10 wt.% NaCl) significantly affected the intrinsic corrosion rate in a nonlinear fashion. The galvanic currents were unaffected by the different salt concentrations.

Keywords: micro-electrochemical cell, mild steel, CO₂ corrosion, weldment

INTRODUCTION

For the oil and gas industry, welding is a fundamental process in the construction of transportation pipelines, production tubing, and other related operational facilities. The welding process connects metallic structures by melting a filler material in between the two structures at high temperature. Carbon steel is by far the most frequently welded metallic material in all heavy industrial applications including the petroleum and petrochemical industry¹. Carbon steel weldment may experience all classical forms of corrosion depending upon the environment to which it is exposed¹. Weldment naturally possess compositional and microstructural heterogeneities, therefore, the corrosion of a weldment appears to be more erratic and is difficult to predict.

According to its special structures, a weldment can be divided into three sections¹: weld metal, heat affected zone (HAZ), and parent metal. A schematic representation of a weldment cut directly from a

*Currently works for Baker Hughes.

©2014 by NACE International.

Requests for permission to publish this manuscript in any form, in part or in whole, must be in writing to NACE International, Publications Division, 1440 South Creek Drive, Houston, Texas 77084.

The material presented and the views expressed in this paper are solely those of the author(s) and are not necessarily endorsed by the Association.

pipeline is shown in Figure 1. The weldment was specially treated with 3% Nital (3% Nitric acid in ethanol) solution to expose the region of the weld and HAZ. It is clearly seen that the parent metal is on the side, the weld metal is in the middle and the heat affected zone is in between.



Figure 1. The weldment specimen etched with 3% Nital (3% Nitric acid in ethanol) solution.

The *weld metal* is the result of melting, which fuses the base metal and filler metal to produce a zone with a composition that is typically different from that of the base metal¹. It is located in the middle of the weldment. The compositional difference could lead to a galvanic couple that may significantly affect the corrosion process of the metal in close proximity to the weld metal.

The *heat affected zone* (HAZ) is the area of the base metal which has experienced extremely intense heat during welding process¹. The heat from the welding process and subsequent re-cooling produce solid-state micro-structural changes in the heat affected zone, which may also alter the corrosion resistance of the affected metal.

The *parent metal* is the base metal which is a certain distance from the weld area and is not affected by the heat brought on by the welding process¹. The metallurgical structure as well as the corrosion resistivity of the parent metal remains unchanged during the welding process.

A weldment can experience different types of corrosion due to this dissimilarity of the metallurgical structures within it. As mentioned before, the compositional difference of the weld and base metal may cause a potential difference and hence lead to a galvanic couple. The galvanic corrosion may significantly accelerate or retard the overall corrosion process. When only the corrosion without galvanic effects is considered, then it is here called intrinsic corrosion. To study the weldment corrosion, intrinsic and galvanic corrosion behaviors have to be considered simultaneously. The combined effects of intrinsic and galvanic corrosion may cause a focus of corrosion attack in a specific location on the weldment, thus lead to severe localized attack. This type of corrosion is also called preferential corrosion of weldment¹.

Preferential weld corrosion of carbon steel has been investigated since 1950s². Studies have shown that preferential weld corrosion is significantly affected by environmental factors³⁻⁶. The morphology and location of preferential weld corrosion in CO₂-containing media are influenced by complex interactions of several parameters, including the environmental (temperature, flow conditions, water composition, pH value, organic acid and partial pressure of CO₂), scaling effects, weld steel composition relative to the parent pipe and welding procedure⁶.

Several issues related to corrosion of carbon steel weldments have been successfully identified in specific cases⁷⁻²⁰; however, problems still exist today in different applications. It is still difficult to predict whether an attack will occur on the HAZ, weld metal or both, in susceptible situations. Corrosion models have not been established to successfully predict the location of weldment corrosion, corrosion rates, and the effectiveness of inhibitors. To better understand the mechanism of weldment corrosion, a study was initiated at the ICMT. This paper describes part of the research that has been done in the past including temperature and chloride concentration effects on weldment corrosion.

EXPERIMENTAL SET UP

All the experiments in this study were conducted in a glass cell under atmospheric pressure conditions. The following paragraphs describe the experimental setup and procedures.

Sample Preparation

A weldment specimen was made from a carbon steel pipe sample that had a weld. All experiments were performed on a “standard weldment” which has no alloying metals in the weld material. The compositions of parent and weld materials are given in Table 1. It appears that there is no significant difference between the compositions of parent and weld material.

Table 1. Elemental analysis (wt.%) of parent metal and filler material of the weldment.

Element	Al	As	C	Co	Cr	Cu	Fe	Mn	Mo	Nb	Ni
Parent	0.037%	0.004%	0.21%	0.002%	0.049%	0.021%	98.3%	1.01%	0.010%	0.010%	0.024%
Weld	0.013%	0.005%	0.12%	0.002%	0.042%	0.046%	98.2%	1.07%	0.013%	0.005%	0.033%
Element	P	S	Sb	Si	Sn	Ta	Ti	V	W	Zn	Zr
Parent	0.013%	0.005%	0.007%	0.27%	0.004%	0.030%	0.003%	0.002%	0.016%	0.001	0.002%
Weld	0.012%	0.007%	0.008%	0.39%	0.004%	0.031%	0.002%	0.003%	0.014%	0.001%	0.003%

Sample segment A wedge shape weldment segment was cut from a pipeline to make a weldment specimen. The machined specimen, prior to separation of weldment segment components, was 35mm long, 8mm wide and 13mm thick. The segment was polished with 150 grit sandpaper on the underside and sides where the weld is exposed. The specimen was then etched with 3% Nital (3% Nitric acid in ethanol) solution to expose the region of the weld and HAZ (as shown in Figure 2). The colored demarcations between weld, HAZ, and parent materials were added after visual observation.



Figure 2. Colored areas of weld and HAZ on the sample image for better visualization. The top of the image would be on the outside of the pipeline while the bottom of the image would be on the inside of the pipeline.

Weldment manufacturing The specimen was cut so that the portions of the weld that would be exposed to the internal pipeline conditions would be used in the experiment. Demarcation lines were drawn using proportional micrometer measurements on the inside pipe wall location of the weld to separate the HAZ material from the weld material and from the parent material on both sides (Figure 3). In order to use the electrochemical noise method, two weld material segments were needed, so an additional weld element was added after the sample was cut in half. After that, wires were soldered to each segment, the segments were arranged in a mold, and then the mold was filled with epoxy. The outer pipe wall portion of the sample was left intact during manufacture of the weldment test sample in order to maintain orientation and spacing, but was removed after potting in epoxy. The six segments were then separated from each other so that external electrical connections could be made to each segment. The finished specimen is shown in Figure 4. Two groups of segments were included in the finished specimen. The reason why is explained in the following paragraphs.



Figure 3. Initial metal cuts in weldment sample to separate parent material from HAZ and HAZ from weld material.

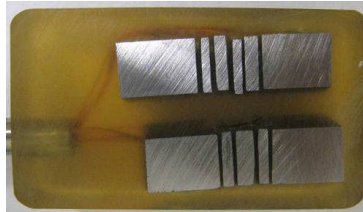


Figure 4. A picture of the weldment sample used in the experiment.

Each weldment surface was polished by silicon carbide sand paper, up to 600 grit, before it was tested. After polishing, the specimen was immersed in an isopropyl alcohol ultrasonic bath for 1 to 2 minutes and then air dried.

Experimental procedure

The experiment was performed in a glass cell as shown in Figure 5. A Saturated Calomel Electrode was used as the reference electrode. The counter electrode was a platinum wire. The glass cell was filled with 2 liters of de-ionized water and the required amount of NaCl to meet the designated chloride ion concentration. Cell temperature was controlled by a hot plate with a thermocouple feedback. Before the test, the solution was deoxygenated by purging with CO₂ gas for 40 minutes to 1 hour. Purging of the glass cell with CO₂ was maintained during the test period. When the desired temperature was obtained, the pH of the test solution was adjusted from equilibrium pH to the desired pH by adding a deoxygenated sodium bicarbonate solution. A weld segment specimen was then placed into the solution and all electrical connections were made externally for electrochemical monitoring.

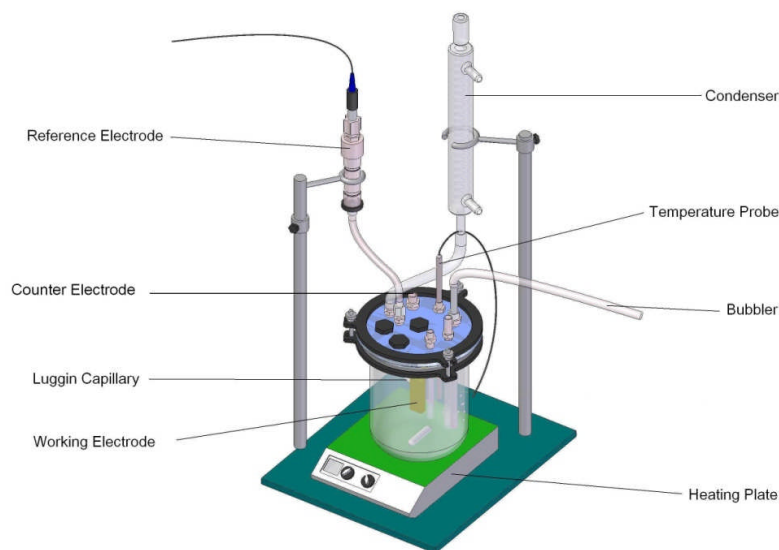


Figure 5. Electrochemical Glass-cell Set-up

Two groups of weld elements were sealed by epoxy in one weldment specimen as shown in Figure 6. One group was always uncoupled throughout the entire test period for linear polarization resistance and potential measurements to observe general intrinsic corrosion rate results without the influence of galvanic corrosion. To simulate the weldment service in reality, the other group was always coupled and would be used to measure the galvanic currents.

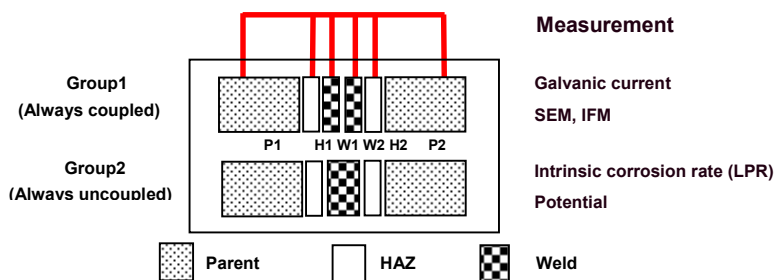


Figure 6. Schematic representation of sample showing coupled segments and uncoupled segments of the weldment with electrochemical measurement methods for each set of segments listed.

RESULTS AND DISCUSSION

The environmental effects including temperature and chloride concentration on weldment corrosion have been investigated in a CO₂ system. The intrinsic corrosion rate of each segment and galvanic current flowing between each segment were measured. Electrochemical noise measurement was also conducted to monitor the possible localized corrosion events. The specimen surface was inspected to support the noise data at different test conditions.

Considering the typical values of anodic Tafel slope (0.04 V/dec) for iron dissolution and cathodic Tafel slope (-0.12 V/dec) for proton and bicarbonate reduction, it would be expected that about 3/4 of the galvanic current relates to changes in the total corrosion rate²¹. The total coupled corrosion rate was obtained from the uncoupled intrinsic corrosion rate and the galvanic current corrosion rate.

The effects of temperature and chloride concentration on the weldment corrosion were studied in the same series of tests. The results are summarized below.

25°C, pH 5.0, 1 bar total pressure, and 1, 5, 10 wt.% NaCl

Experimental data were shown in three categories: intrinsic corrosion rate, galvanic corrosion rate and surface analysis.

Intrinsic Corrosion Rates The LPR intrinsic corrosion rates of uncoupled parent, HAZ, and weld materials with time at 25°C, different chloride concentrations (1, 5 or 10 wt.% NaCl) are shown in Figure 7, Figure 8, and Figure 9 respectively. It appears that the intrinsic corrosion rate does not vary significantly for the various segments. The steady increase over time is due to the development of the iron carbide (cementite) layer which is actually the uncorroded portion of the steel. The chloride concentration effects on the intrinsic corrosion rate are summarized in Table 2. It is clearly seen that the intrinsic corrosion rate of each segment did not change significantly when salt concentration was changed from 1 wt.% to 5 wt.%. However, when salt concentration was further increased to 10 wt.%, corrosion rates of all three segments decreased. This may be due to the absorption of chloride ions on the steel surface, thus slowing down the corrosion by limiting the surface area available to corrosive species²².

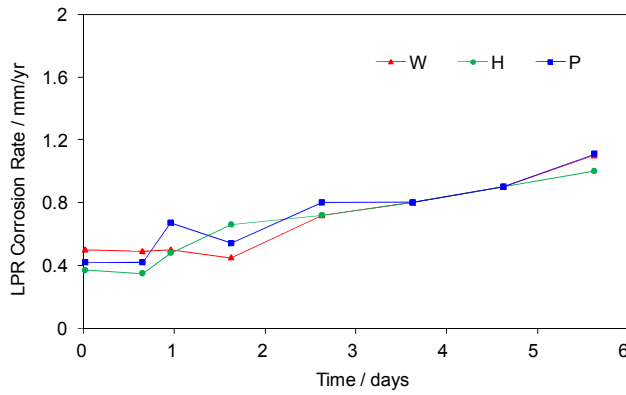


Figure 7. Intrinsic corrosion rate of uncoupled weldment vs. time at 1 wt.% NaCl, 25°C.

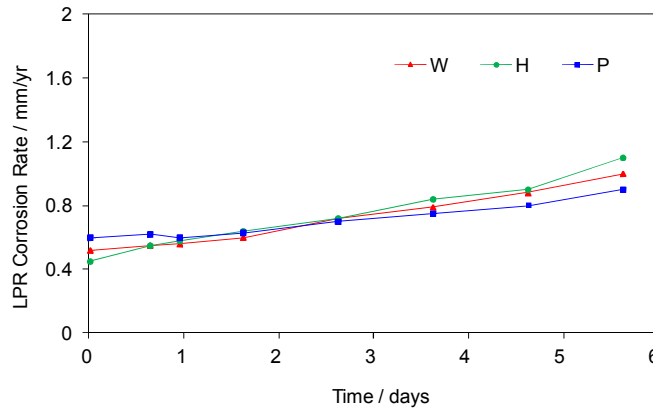


Figure 8. Intrinsic corrosion rate of uncoupled weldment vs. time at 5 wt.% NaCl, 25°C.

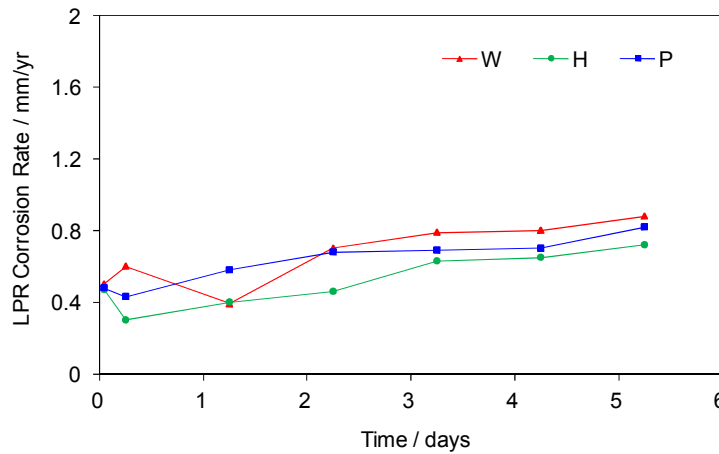


Figure 9. Intrinsic corrosion rate of uncoupled weldment vs. time at 10 wt.% NaCl, 25°C.

Table 2. Average intrinsic corrosion rates of weldment segments at 25°C (P = parent metal, H = heat affected zone metal, W = weld metal).

	1 wt.% NaCl			5 wt.% NaCl			10 wt.% NaCl		
	P	H	W	P	H	W	P	H	W
Average intrinsic corrosion rate (mm/yr)	0.74	0.71	0.71	0.71	0.75	0.73	0.65	0.52	0.68

Galvanic Currents The galvanic current measurement results of coupled segments at different salt concentrations are shown in Figure 10, Figure 11, and Figure 12. According to the test results, it appears that parent and weld metal did not show consistent polarity. However, considering the total testing time (6 days), the weld metal tends to exhibit anodic behavior with respect to the other segments while the HAZ is the neutral section. For the same testing time, the parent steel was the more noble metal acting as a cathode. The test results also show that the galvanic current of the weld metal was about $4 \mu\text{A}$ and the galvanic current of the parent metal was around $-4 \mu\text{A}$. The increase of chloride concentration from 1 wt.% to 5 wt.% and 10 wt.% does not appear to affect the magnitude and polarity of the galvanic currents.

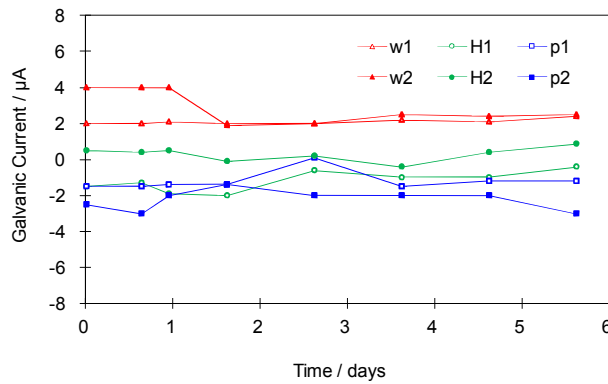


Figure 10. Galvanic current of coupled weldment vs. time at 1 wt.% NaCl, 25°C.

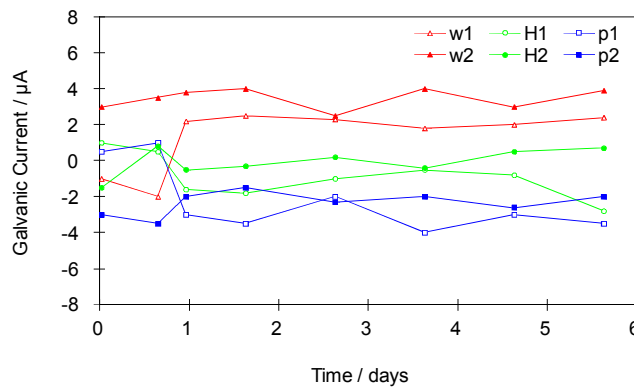


Figure 11. Galvanic current of coupled weldment vs. time at 5 wt.% NaCl, 25°C.

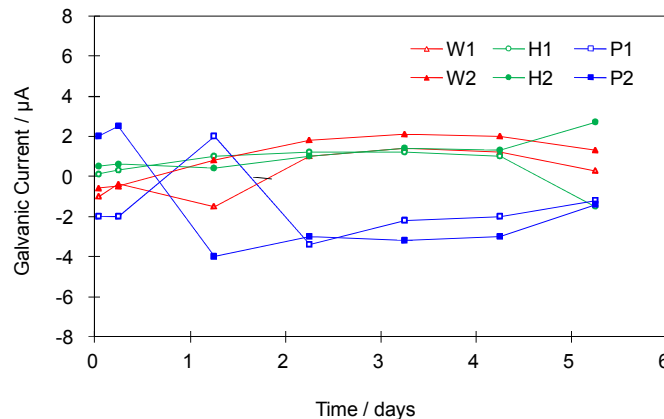


Figure 12. Galvanic current of coupled weldment vs. time at 10 wt.% NaCl, 25°C.

©2014 by NACE International.

Requests for permission to publish this manuscript in any form, in part or in whole, must be in writing to NACE International, Publications Division, 1440 South Creek Drive, Houston, Texas 77084.

The material presented and the views expressed in this paper are solely those of the author(s) and are not necessarily endorsed by the Association.

The galvanic effects on the total corrosion rate of each segment of weldment are also clarified by comparing them with the intrinsic corrosion rate results. The calculated total corrosion rates of the parent metal, the HAZ metal, and the weld metal at 1 wt. % NaCl, 25°C are shown in Figure 13, Figure 14, and Figure 15 respectively. It appears that the corrosion of parent metal as well as HAZ was mitigated by the galvanic effect. On the other hand, the galvanic effect accelerated the corrosion of weld metal. However, the magnitude of galvanic currents at all test conditions is relatively small; consequently, the galvanic current did not affect the total corrosion process significantly. As shown earlier, chloride ions did not show a considerable effect on the magnitude of galvanic current.

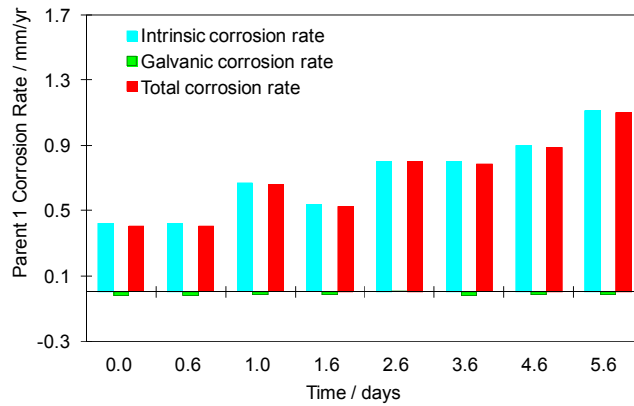


Figure 13. Corrosion rate of Parent 1 metal compared to the intrinsic corrosion rate and galvanic corrosion rate at 1 wt.% NaCl, 25°C.

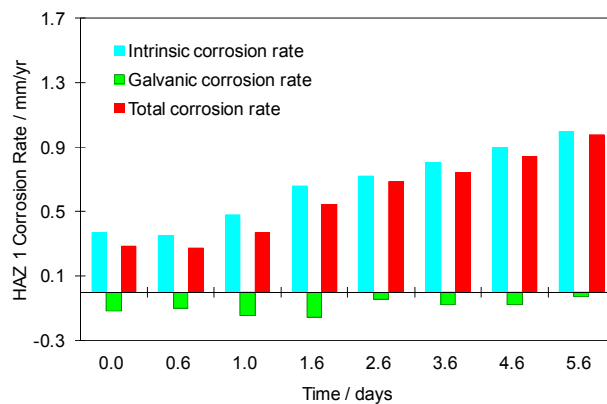


Figure 14. Corrosion rate of HAZ 1 metal compared to the intrinsic corrosion rate and galvanic corrosion rate at 1 wt.% NaCl, 25°C.

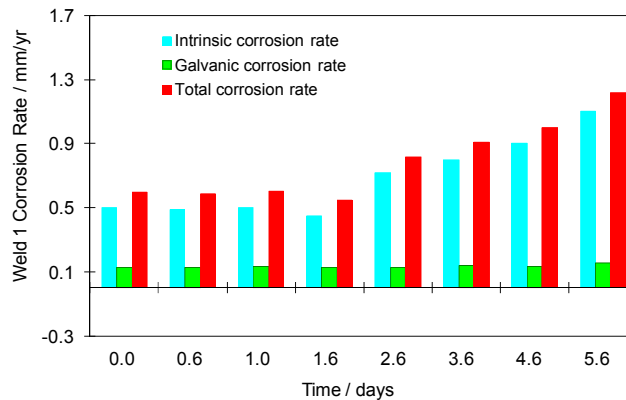


Figure 15. Corrosion rate of weld 1 metal compared to the intrinsic corrosion rate and galvanic corrosion rate at 1 wt.% NaCl, 25°C.

Surface Analysis The specimen surface was scanned by SEM after the experiment. The surface morphologies of the parent, the HAZ, and the weld metal surface (with film) after different chloride concentration tests are shown in Figure 16, Figure 17, and Figure 18. No evidence of localized attack on any of the weldment segment surfaces was detected.

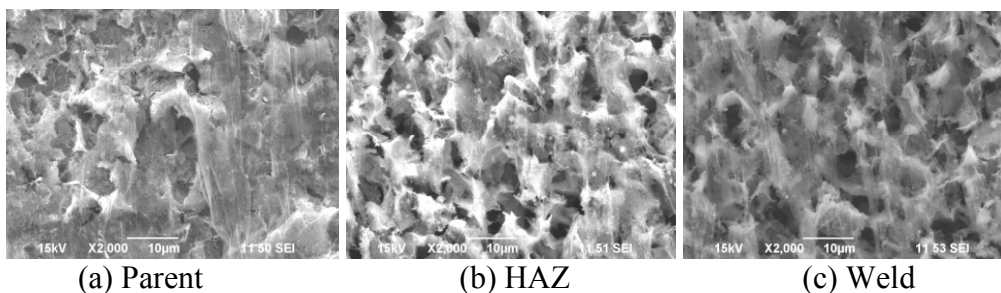


Figure 16. Surface morphology (with film) of parent, HAZ, and weld after 6 days at 1 wt.% NaCl, 25°C.

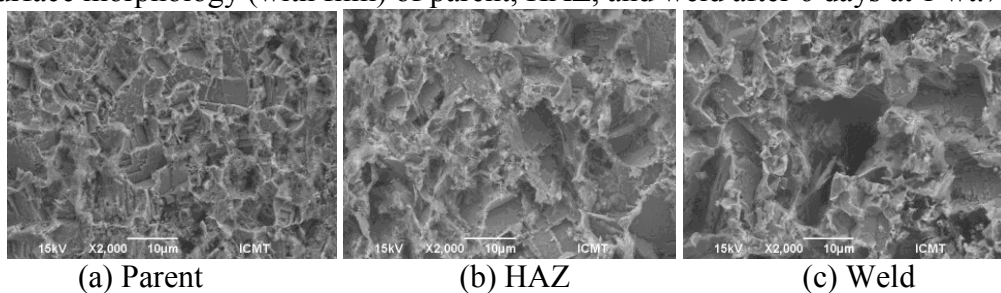


Figure 17. Surface morphology (with film) of Parent, HAZ, and Weld after 6 days at 5 wt.% NaCl, 25°C.

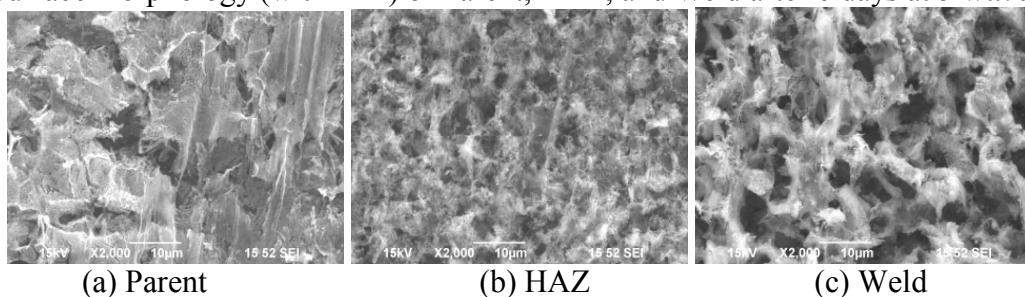


Figure 18. Surface morphology (with film) of parent, HAZ, and weld after 6 days at 10 wt.% NaCl, 25°C.

60°C, pH 5.0, 1bar total pressure, and 1, 5, 10 wt.% NaCl

Similar experiments were conducted at 60°C. The experimental results are shown below.

Corrosion rates The intrinsic corrosion rates of uncoupled parent, HAZ, and weld materials with time measured by LPR at 60°C, pH 5 and 1, 5 or 10 wt.% NaCl are shown in Figure 19, Figure 20, and Figure 21 respectively. The results suggest that the intrinsic corrosion rates of parent, HAZ, and weld material are of the same magnitude under the same test conditions. The chloride effects on intrinsic corrosion rate are shown in Table 3. Different from the results at 25°C, it appears that an increase of chloride concentration from 1 wt.% to 5 wt.% at 60°C significantly increased the intrinsic corrosion rates of all segments. When the chloride concentration further increased from 5 wt.% to 10 wt.%, the acceleration of corrosion rate did not persist. The experimental results suggest that the interaction of the chloride ions with the steel surface at high temperature may be significantly different from the interaction at low temperatures.

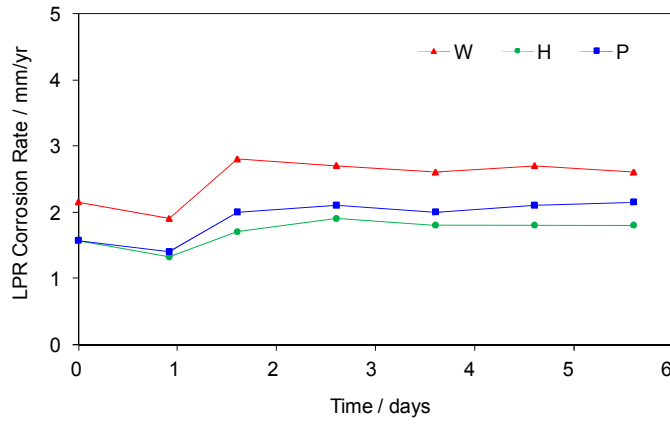


Figure 19. LPR corrosion rate of uncoupled weldment vs. time at 1 wt. % NaCl, 60°C.

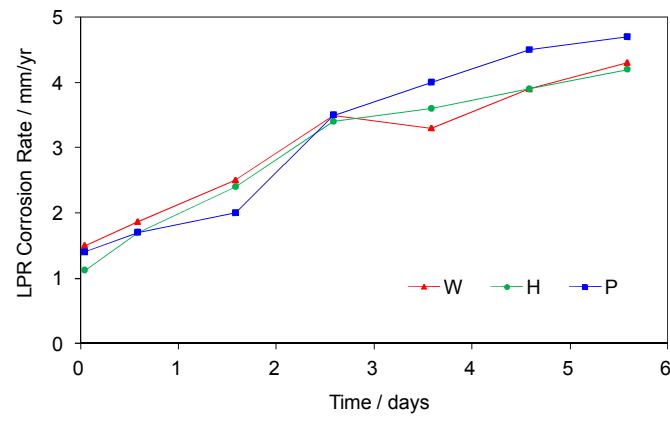


Figure 20. LPR corrosion rate of uncoupled weldment vs. time at 5 wt.% NaCl, 60°C.

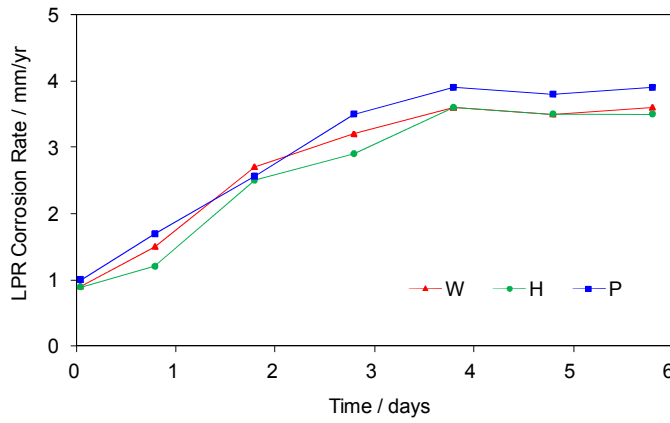


Figure 21. LPR corrosion rate of uncoupled weldment vs. time at 10 wt.% NaCl, 60°C.

Table 3. Average intrinsic corrosion rates of weldment segments at 60°C.

	1 wt% NaCl			5 wt% NaCl			10 wt% NaCl		
	P	H	W	P	H	W	P	H	W
Average intrinsic corrosion rate (mm/y)	1.93	1.72	2.53	3.26	3.07	3.1	3.05	2.72	2.86

Galvanic Currents The galvanic currents flowing between each segment at 60°C were also measured. The results at different salt concentrations are shown in Figure 22, Figure 23, and Figure 24. According to the test results, the galvanic current on weld metal was always positive, which suggests that the weld metal acting as anode was always more active than the HAZ and the parent metal. The HAZ appears to be the neutral section and the parent metal was the section that was cathodically protected. The result also shows that the magnitude of galvanic current on weld metal increased from 4 μA to around 20 μA when temperature was increased from 25°C to 60°C. However, the chloride ion concentration does not appear to have a significant effect on the magnitude of the galvanic current and the metal polarity at 60°C, which was observed at 25°C as well.

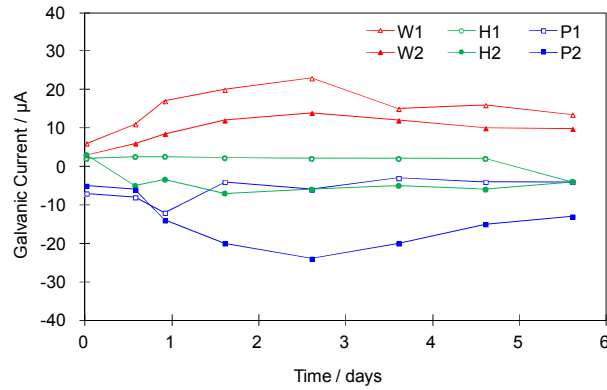


Figure 22. Galvanic current of coupled weldment vs. time at 1 wt.% NaCl, 60°C.

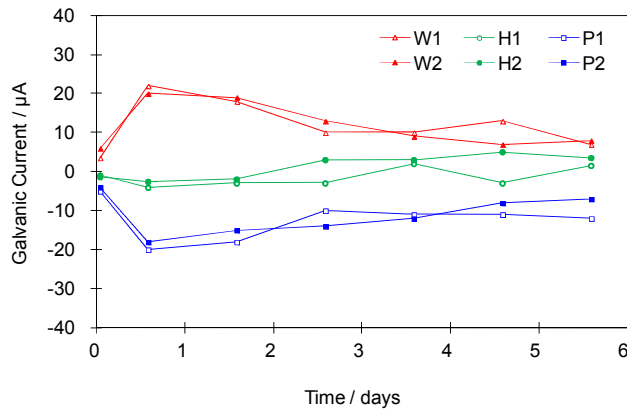


Figure 23. Galvanic current of coupled weldment vs. time at 5 wt.% NaCl, 60°C.

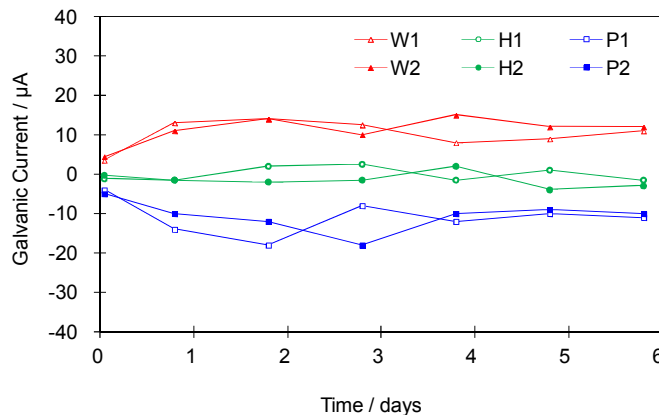


Figure 24. Galvanic current of coupled weldment vs. time at 10 wt.% NaCl, 60°C.

The total corrosion rates of each segment of weldment which combines the intrinsic and the galvanic corrosion rate at 1 wt.% NaCl and 60°C are shown in Figure 25, Figure 26, and Figure 27. Apparently, the total corrosion rate of the parent metal was reduced by the galvanic effect. The galvanic current significantly accelerated the total corrosion rate of the weld metal.

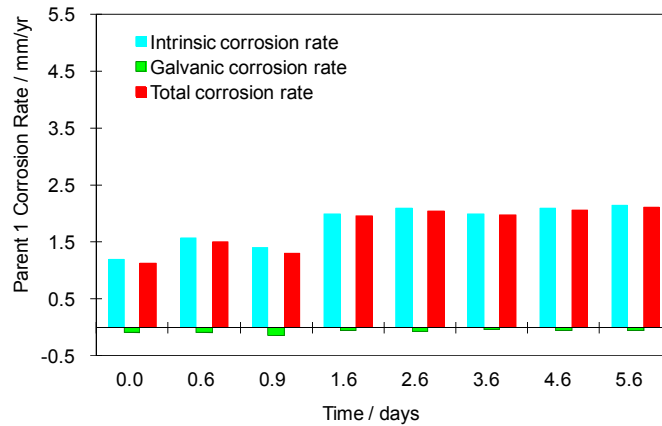


Figure 25. Corrosion rate of parent 1 metal compared to the intrinsic corrosion rate and galvanic corrosion rate at 1 wt.% NaCl, 60°C.

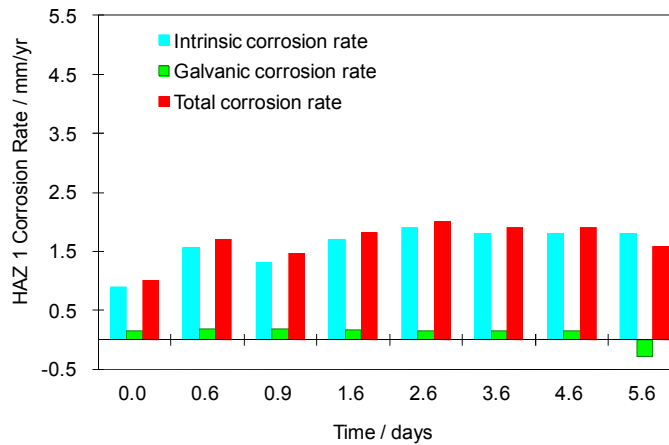


Figure 26. Corrosion rate of HAZ 1 metal compared to the intrinsic corrosion rate and galvanic corrosion rate at 1 wt.% NaCl, 60°C.

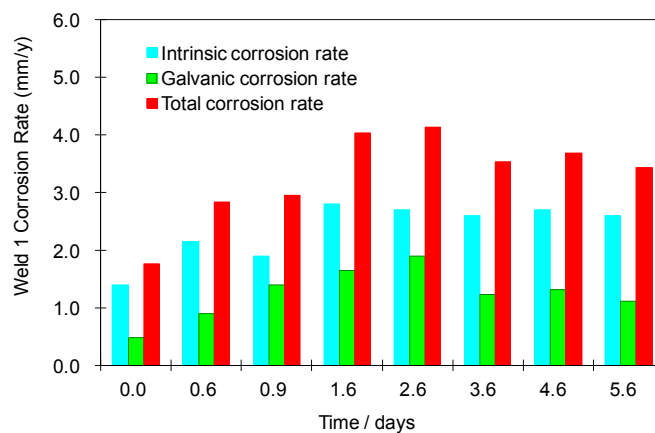


Figure 27. Corrosion rate of weld 1 metal compared to the intrinsic corrosion rate and galvanic corrosion rate at 1 wt.% NaCl, 60°C.

Surface Analysis The surface morphologies of parent, HAZ, and weld metal (with corrosion products) after experiments at different chloride concentrations are shown in Figure 28, Figure 29 and Figure 30. A crystallized corrosion product was detected on the specimen surface under the condition of 1 wt.% NaCl, 60°C. The EDX analysis as shown in Figure 31 confirms it to be iron carbonate. However, when the salt concentration was increased to 5 and 10 wt.%, the formation of iron carbonate on the coupon surface was hardly observable by SEM. The iron carbonate layer was then removed by Clarke solution²³. The surface morphology is shown in Figure 32. Localized corrosion was not observed on the surfaces of all segments. Based on the experimental results, even when the galvanic effects were accelerated by an increase of temperature, localized corrosion event was still not observed at all chloride concentrations.

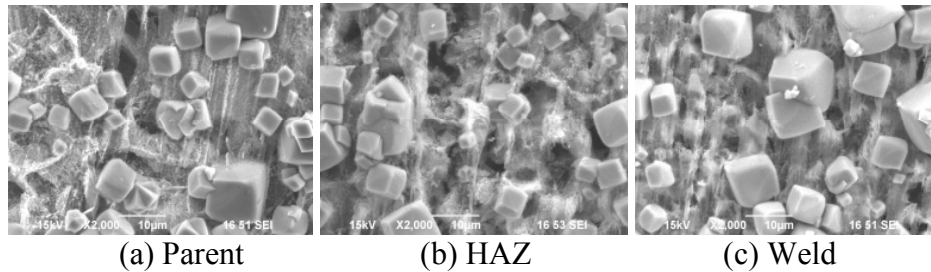


Figure 28. Surface morphology (with corrosion products) of parent steel, HAZ, and weld after 6 days at 1 wt.% NaCl, 60°C.

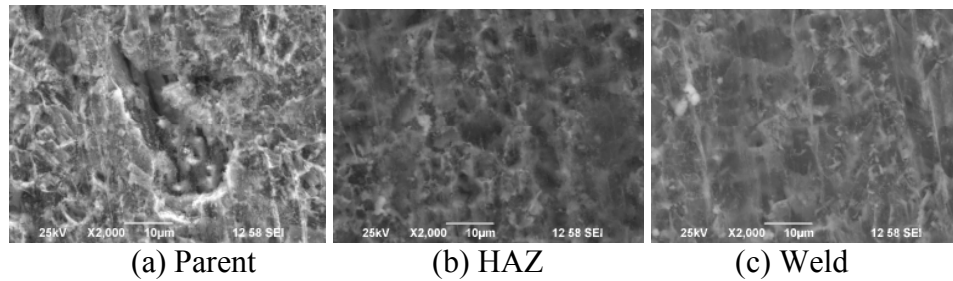


Figure 29. Surface morphology of parent steel, HAZ, and weld after 6 days at 5 wt.% NaCl, 60°C.

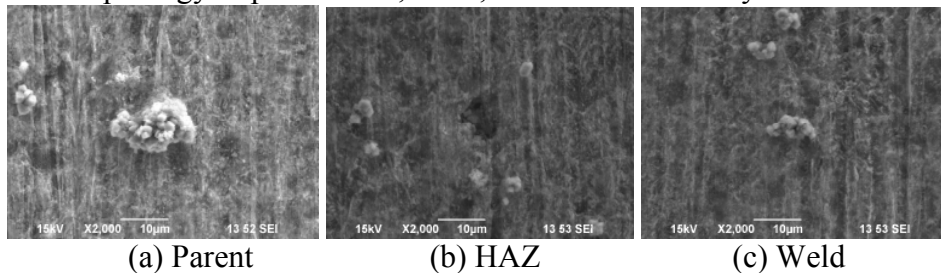


Figure 30. Surface morphology of parent steel, HAZ, and weld after 6 days at 10 wt.% NaCl, 60°C.

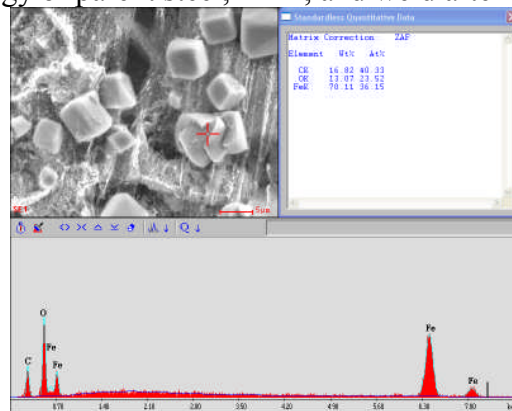


Figure 31. EDX results of crystals on parent steel after 6 days at 1 wt.% NaCl, 60°C.

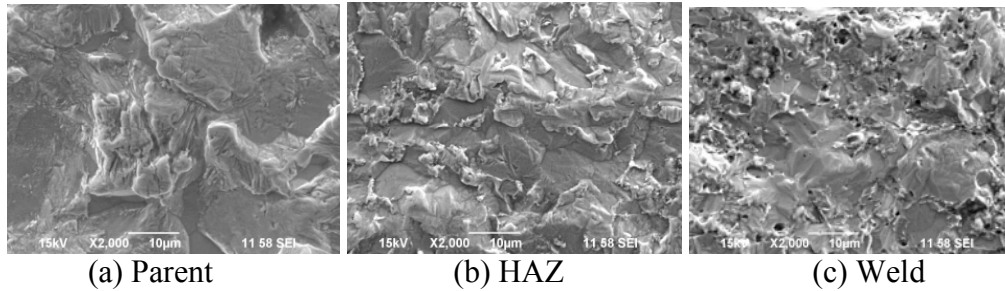


Figure 32. Surface morphology (without crystals) of parent steel, HAZ, and weld after 6 days at 1 wt.% NaCl, 60°C.

CONCLUSIONS

Temperature and chloride ion concentration effects were studied in this series of experiments. An increase of temperature from 25°C to 60°C significantly increased the intrinsic corrosion rate of each segment. The magnitude of galvanic current flowing through each segment was also increased by an increase of temperature.

At 25°C, an increase of chloride concentration from 5 wt.% to 10 wt.% reduced the intrinsic corrosion rate of each segment. This may be due to the absorption of chloride ions on the steel surface acting as a mass transfer barrier. However, when the temperature was increased to 60°C, the effects of chloride ion concentration on the intrinsic corrosion rate were opposite, i.e., the intrinsic corrosion rate was increased with an increase of chloride concentration.

The intrinsic corrosion rate of each segment appears to have no significant difference from each other under the same experimental conditions. The weldment metal always appears to be anodic with respect to HAZ and parent metal.

No localized corrosion was observed at all test conditions.

Reference

1. J. Davis, Corrosion of Weldments, ASM International, 2006.
2. G. A. Nelson, "Prevention of Localized Corrosion in Sulfuric Acid Handling Equipment", Corrosion, Vol. 14, No. 3, 1958, pp. 45-50.
3. S. Turgoose, J. Palmer, G. Dicken, "Preferential Weld Corrosion of 1% Ni Welds: Effect of Solution Conductivity and Corrosion Inhibitors", Corrosion/05, Paper No. 05275, NACE International, Houston, Texas, 2005.
4. E. Gulbrandsen, A. Dugstad, "Corrosion Loop Studies of Preferential Weld Corrosion and Its Inhibition in CO₂ Environments", Corrosion/05, Paper No. 05276, NACE International, Houston, Texas, 2005.
5. D. Queen, C. Lee and J. Palmer, "Guidelines for the Prevention, Control and Monitoring of Preferential Weld Corrosion of Ferritic Steel in Wet Hydrocarbon Production Systems Containing CO₂", SPE, Paper No. 87552, 2004.
6. S. Olsen, B. Sundfer and J. Enerhaug, "Weld Corrosion in C-steel Pipelines in CO₂ Environments- Comparison between Field and Laboratory Data". Corrosion/97, Paper No.43, NACE International, Houston, Texas, 1997.
7. C. Lee, S. Bond, and P. Woollin, "Preferential Weld Corrosion: Effects of Weldment Microstructure and Composition", Corrosion/05, Paper No. 05276, NACE International, Houston, Texas, 2005.

©2014 by NACE International.

Requests for permission to publish this manuscript in any form, in part or in whole, must be in writing to NACE International, Publications Division, 1440 South Creek Drive, Houston, Texas 77084.

The material presented and the views expressed in this paper are solely those of the author(s) and are not necessarily endorsed by the Association.

8. P. I. Nice and ó Strandmyr, "Materials and Corrosion Control Experience within the Statfjord Field Seawater Injection Systems", Corrosion/93, Paper No. 64, NACE International, Houston, Texas, 1993.
9. J. W. Palmer, J. L. Dawson, T. Ulrich and A.N. Rothwell, "Inhibition of Weld Corrosion under Flowing Conditions – the Development of Test Procedures", Corrosion/93, Paper No. 119, NACE International, Houston, Texas, 1993.
10. R. J. Pargeter and T.G. Gooch, "Welding C-Mn Steels for Sour Service", Corrosion/95, Paper No. 63, NACE International, Houston, Texas, 1995.
11. T. Hodgkiess, N. Eid and W.T. Hanbury, "Corrosion of Welds in Seawater", Desalination, Vol. 27, No. 2, 1978, pp. 129–136.
12. A. N. Rothwell, "Weld Corrosion: Causes and Solutions", Corrosion Prevention and Control, Vol. 39, 1992, pp. 113.
13. M. W. Joosten and G. Payne, "Preferential Corrosion of Steel in CO₂ Containing Environments", Corrosion/88, Paper No. 211, NACE International, Houston, Texas, 1988.
14. V. S. Voruganti, H. B. Luft, D. DeGreer and S. A. Bradford, "Scanning Reference Electrode Technique for the Investigation of Preferential Corrosion of Weldments in Offshore Applications", Corrosion, Vol. 47, No. 5, 1991, pp. 343.
15. M. Eashwar and S. C. Dexter, "Relation of Bacterial Settlement Patterns to Anodic Activity on Stainless Steel Weldments", Corrosion/99, Paper No. 174, NACE International, Houston, Texas, 1999.
16. H. Ogawa, Y. Tomoe, T. Hara, A. Sakamoto, "A Case Study of the Uneven Corrosion of A Choke Valve at A Gas-well Head", Corrosion/2000, Paper No. 4, NACE International, Houston, Texas, 2000.
17. I. G. Winning, D. McNaughtan, N. Bretherton, and A. J. McMahon "Evaluation of Weld Corrosion Behavior and the Application of Corrosion Inhibitors and Combined Scale/Corrosion Inhibitors", Corrosion/04, Paper No. 04538, NACE International, Houston, Texas, 2004.
18. F. Gui, D. Hill, C. Kang, and C. Joia, "Inhibition of Galvanic Corrosion of Carbon Steel and Nickel Alloy in Oil and Gas Production Applications", Corrosion/2010, Paper No. 10333, NACE International, Houston, Texas, 2010.
19. M. Sephton and P.C. Pistorius, "Localized Corrosion of Carbon Steel Weldments", Corrosion, Vol. 56, No. 12, 2000.
20. D. McNaughtan and I.G. Winning, "Comparison of Segmented Weld Corrosion Tests with Short and Long Pre-corrosion and the Influence of Synergist in Corrosion Inhibitors", SPE/04, Paper No. 87553, Society of Petroleum Engineers, 2004.
21. L. Huang, "Investigation of the Environmental Effects on Intrinsic and Galvanic Corrosion of Mild Steel", Master thesis, Ohio University, 2012
22. C.Garcia, F. Martin, P.de Tiedra, Y. Blanco and M. Lopez, "Pitting Corrosion of Welded Joints of Austenitic Stainless Steels Studied by Using an Electrochemical Minicell", Corrosion Science, Vol.50, 2008, pp.1184-1194.
23. ASTM G1 – 81, (Section 7)," Standard Practice for Preparing, Cleaning, and Evaluating Corrosion Test Specimens," Proceedings of the Symposium on Laboratory Corrosion Tests and Standards, G. S. Haynes, R. Balboian, editors, pp. 505-510, 1983.